ELSEVIER

Thin Solid Films 388 (2001) 201–207

thin solid films

www.elsevier.com/locate/tsf

Electrodeposition of Cu–Re alloy thin films

R. Schrebler[a], M. Merino[a], P. Cury[a], M. Romo[a], R. Córdova[a], H. Gómez[a], E.A. Dalchiele*[,b]

[a] *Instituto de Química, Facultad de Ciencias, Universidad Católica de Valparaíso, Casilla 4059, Valparaíso, Chile*
[b] *Instituto de Física, Facultad de Ingeniería, Herrera y Reissig 565, C.C. 30, 11000 Montevideo, Uruguay*

Received 19 November 1999; received in revised form 2 January 2001; accepted 7 February 2001

Abstract

The electrodeposition of copper–rhenium alloys from Cu(II) and Re(IV) solutions was studied in an aqueous H_2SO_4 matrix. Different substrates have been used (glassy carbon, titanium and gold), and the effect of them on the electrochemical behavior of the studied ions is shown. Cyclic voltammetry was used in conjunction with oscillating quartz crystal nanogravimetry to delineate features in the voltammograms accompanied by mass loss or gain at the electrode surface, from those attributable to the solution phase. The obtained Cu–Re films were subjected to scanning electron microscopy (SEM), energy dispersive X-ray analysis (EDX) and X-ray diffraction analysis (XRD). The rhenium content increases as the potential was made more cathodic, reaching a maximum value of 10% atomic composition. The films were amorphous with a cauliflower structure. © 2001 Published by Elsevier Science B.V. All rights reserved.

JEL classifications: 81.15.P; 61.43.D; 68.55.J.-

Keywords: Alloys; Electrochemical deposition; X-Ray diffraction; Nanobalance

1. Introduction

Although some research has been dedicated to investigating the possibility of producing binary rhenium alloys by electrodeposition, i.e. Co–Re [1–3], Ni–Re [4]; little is published on electrodeposition of Cu–Re alloys. To our knowledge the first report on electrodeposition of Cu–Re alloys is that of Nikitina et al. [5], in which metallic deposits of Cu–Re alloy (containing up to 30% copper), were made by use of direct and intermittent current from an electrolyte containing perrhenate and copper ions. In an earlier work [6], co-electrodeposited copper–rhenium on polypyrrole electrodes in alkaline media were obtained in order to study the electrochemical nitrate reduction.

Therefore, we undertook an investigation on the electrodeposition of copper–rhenium alloys, the results of which are reported in the present paper. Three main techniques have been used in order to find the suitable growth conditions for the alloy: cyclic voltammetry, nanogravimetry studies (in situ electrochemical quartz crystal nanobalance, EQCN), and potential step experiments. The cyclic voltammetry determines the potential ranges where the redox processes of interest are taking place [7]. The electrochemical quartz crystal nanobalance is an excellent and very useful tool for the study of the early stages of metal deposition on a foreign substrate [8,9]. This technique allows us to follow the mass of the species that are being deposited, adsorbed or those that are leaving the interface. Fi-

* Corresponding author. Fax: +598-2-711-1630.
E-mail address: dalchiel@fing.edu.uy (E.A. Dalchiele).

PII: S0040-6090(01)00850-1

nally, the potential step experiments, as a technique, are very useful in the nucleation and growth studies of metals [10,11]. They were supplemented by ex situ characterization techniques: X-ray diffraction, scanning electron microscopy (SEM) and composition analysis.

2. Experimental

The electrochemical experiments were carried out in a three-compartment three-electrode glass cell. The working electrodes were glassy carbon, copper and titanium discs, of area 0.07 cm^2. The gold working electrode was a polycrystalline thin film deposited onto quartz resonator (ELCHEMA) with a geometric area of 0.23 cm^2. An AT-cut quartz crystal resonating at a fundamental frequency of 10 MHz was employed in this study. The particular crystal had a mass sensitivity of 5.8 ng cm^{-2} Hz^{-1}. Thus monolayer coverage of Cu at the Au surface corresponding to a frequency change of 33 Hz, and a mass increase of 191 ng cm^{-2} is routinely measurable by the EQCN-ELCHEMA instrument which has a nominal detection limit of approximately 1 Hz. Before each experiment the gold electrode was cleaned with a freshly prepared H_2SO_4–HNO_3 (1:1) mixture for 2 min. Then this crystal face was extensively rinsed with Milli-Q water and finally dried with argon. Other electrodes were polished with alumina slurry (particle size, 0.3 μm) and then washed thoroughly with Milli-Q water and sonicated for 2 min. The reference electrode was a saturated calomel electrode (SCE). All potential values in this paper are reported vs. the SCE. The counter-electrode was a Pt coil.

The electrodeposition experiments were carried out in an aqueous bath containing 6.25 mM $CuSO_4$ + 0.1 M Na_2SO_4 (solution A); 50.0 mM $HReO_4$ + 0.1 M Na_2SO_4 (solution B) or 6.25 mM $CuSO_4$ + 50.0 mM $HReO_4$ + 0.1 M Na_2SO_4 (solution C). The pH adjustment was done by adding sulfuric acid. All the reagents employed were Merck p.a. Argon was flushed through the cell and the electrolyte prior to the experiments, and an argon flow was maintained over the solution during the measurements.

The E–t programs applied to the electrode were as follows: the potential was first switched from +0.8 V and maintained for 2 min, in order to clean the electrode surface. Electrodeposition was carried out by further step to a potential between −0.15 V and −0.75 V which are referred to as the electrodeposition potential E_e. For the stripping analyses, 0.5 M H_2SO_4 (solution D) was employed as the stripping media and the sweep rate was in all cases 0.020 V s^{-1}.

The voltammetry and chronoamperometric experiments were done with a PINE (Pine Instrument Company, Model RDE4) potentiostat system and the mass measurements were carried out in an electrochemical quartz nanobalance ELCHEMA (system EQCN-501). All the experiments were carried out at a controlled temperature of 25°C ± 0.05°C, under an argon atmosphere.

Scanning electron microscopy (SEM) pictures were obtained on a Philips XL 40 LaB_6 apparatus. Quantitative standardless microanalyses were obtained using an energy dispersive X-ray analysis (EDX) PV 99 X-ray spectrometer equipped with a thin Be window. ZAF corrections (taking into account the factors of atomic number Z, absorption A, and fluorescence correction F) were made to quantitative measurements, taken with an accelerating voltage of 25 keV. The structures of the films were examined by X-ray diffraction analysis, on a Philips PW3710 instrument (Cu–K_α radiation, 40 kV and 30 mA, narrow divergence slit of 1/6°).

3. Results and discussion

Figs. 1–3 show a set of E/I potentiodynamic profiles corresponding to the different studied interfaces, i.e. at a glassy carbon (Fig. 1), titanium (Fig. 2) and gold (Fig. 3) electrode in 0.1 M Na_2SO_4, pH 2 containing either 6.25 mM $CuSO_4$, 50 mM $HReO_4$ or 6.25 mM $CuSO_4$ + 50 mM $HReO_4$. The voltammetry scans were initiated at 0.9 V in the cathodic sense, at 0.005 V s^{-1}. Thus, consideration of these voltammetry curves reveals that two cathodic processes are involved: those associated with the electrodeposition of copper (I_c) and rhenium (II_c), respectively. On the other hand, during the anodic scan, two stripping waves corresponding to copper (I_a) and rhenium (II_a) are observed. Furthermore, in the cyclic voltammetric curve obtained onto a glassy carbon electrode (see Fig. 1), the presence of a shoulder at the anodic side of the rhenium stripping peak (II_a) can be seen. This anodic shoulder corresponds to the stripping of a first layer with special properties due to the carbon rhenium interface, according to the current–time transients of rhenium onto glassy carbon (see below). Thus it appears that it is easier to dissolve electrochemically deposited rhenium when coated on rhenium, than this particular layer. This is not observed for copper, as expected close to peak I_a, in the same experiment. However, as shown in Fig. 3, this shoulder is observed for copper when the cyclic voltammetry experiments are done onto a gold electrode. It is well know that copper can be deposited at underpotential (u.p.d.) onto gold substrates. So, as it was discussed for rhenium onto glassy carbon, the small observed peak must correspond to dissolution of an underpotential copper first layer. In the case of the cyclic voltammetries studies done onto a titanium electrode (see Fig. 2), both copper and rhenium present a shoulder at more anodic potentials, in their corresponding anodic waves. The titanium electrode is always covered with a native oxide film, which can interact with the first layer of the metal.

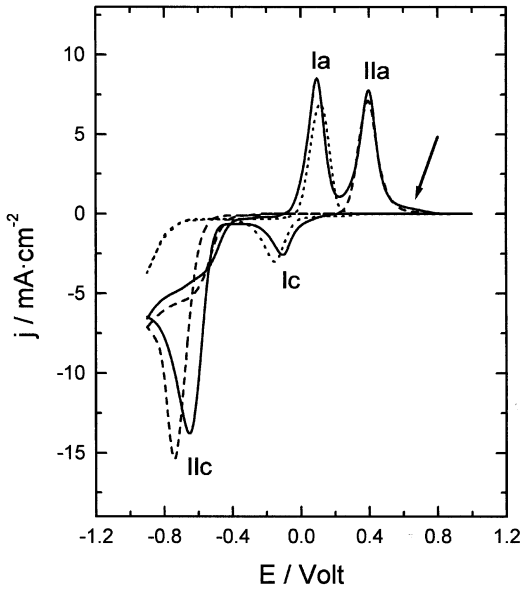

Fig. 1. Cyclic voltammogram for a glassy carbon electrode in 6.25 mM $CuSO_4$ (···), in 50 mM $HReO_4$ (-----) and in 6.25 mM $CuSO_4$ + 50 mM $HReO_4$ (———), supporting electrolyte 0.1 M Na_2SO_4 at pH 2. Scan rate, 5 mV s^{-1}. The arrow denotes the shoulders in the stripping anodic currents, see explanation in the text.

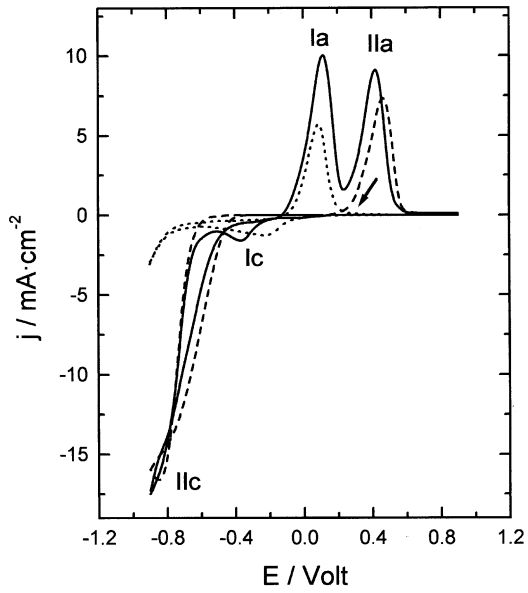

Fig. 3. Cyclic voltammogram for a gold electrode in 6.25 mM $CuSO_4$ (···), in 50 mM $HReO_4$ (-----) and in 6.25 mM $CuSO_4$ + 50 mM $HReO_4$ (———), supporting electrolyte 0.1 M Na_2SO_4 at pH 2. Scan rate, 5 mV s^{-1}. The arrow denotes the shoulder in the stripping anodic current, see explanation in the text.

Thus it seems possible that in this oxide interface, intermediate oxidation states of copper and rhenium species (Cu_2O, Re_2O_3, ReO_2), can be stabilized during the anodic scan. The presence of a nucleation loop on the return scan is also unmistakable.

On titanium electrodes it is very difficult to eliminate the native oxide film, which passivates the electrode surface. For this reason, the oxide film resistance deforms the voltammetric responses. Furthermore, besides these ohmic differences observed, mainly when titanium is used as a substrate; the electric response of the electrodeposition process of Cu and Re are affected by diverse factors that depend on the presence of both species (Cu^{+2} and ReO_4^-) in the electrolytic bath, and by the nature of the metallic substrate on which the electrodeposition is made. For example, at the glassy carbon (Fig. 1) and at the titanium (Fig. 2) electrodes, a slight anodic shift in the peak potential I_c and II_c can be observed when both species are present in the electrolytic solution. At the same time, we can observe a decrease of the charge associated with peak II_c when Re is electrodeposited together with copper. This last phenomenon can be attributed to the minor contribution of the hydrogen evolution reaction when rhenium is co-deposited together with copper.

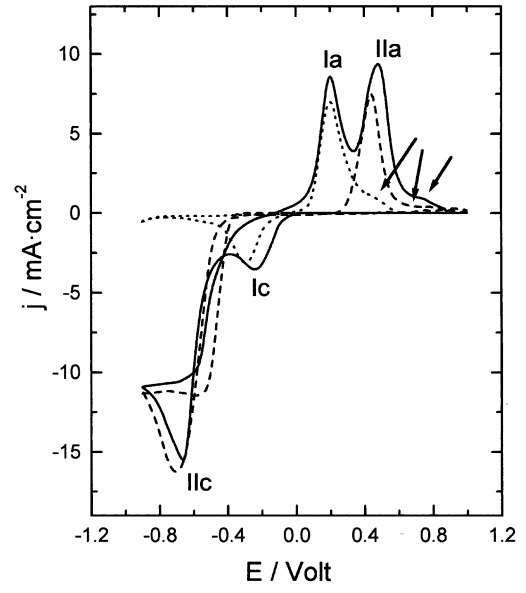

Fig. 2. Cyclic voltammogram for a titanium electrode in 6.25 mM $CuSO_4$ (···), in 50 mM $HReO_4$ (-----) and in 6.25 mM $CuSO_4$ + 50 mM $HReO_4$ (———), supporting electrolyte 0.1 M Na_2SO_4 at pH 2. Scan rate, 5 mV s^{-1}. The arrows denote the shoulders in the stripping anodic currents, see explanation in the text.

On the other hand, at the gold electrode a shift of the peak potential I_c can be seen towards more negative values when the ReO_4^- ion is present in the electrolytic bath. This phenomenon can be explained if we consider that the ReO_4^- ion could be adsorbed onto the electrode surface in the potential region previous to the copper electrodeposition.

Use of nanogravimetry in conjunction with sweep potential experiments aids considerably in the interpretation of the Au voltammetry data. Fig. 4 shows the mass changes with potential at Au electrode (a′, b′) superimposed on voltammetric scans (a,b) in an electrolyte bath with copper and copper + rhenium ions,

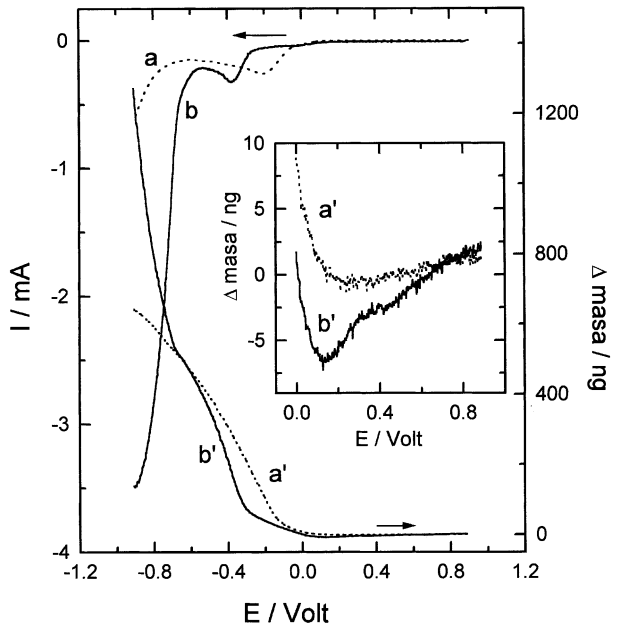

Fig. 4. Cyclic voltammograms (a and b curves, potential scan rate: 10 mV s^{-1}) and nanogravimetry scans (a′ and b′ curves, potential scan rate: 10 mV s^{-1}) at a gold electrode in 6.25 mM $CuSO_4$ (···) and in 6.25 mM $CuSO_4$ + 50 mM $HReO_4$ (———) solutions, supporting electrolyte 0.1 M Na_2SO_4 at pH 2. The inset shows a zoom of the nanogravimetry scan in the 0.0–0.8 V region.

respectively. The inset of Fig. 4 shows a mass loss (curve b′) that can be attributed to the desorption of the ReO_4^- ion as the potential is made more cathodic. Furthermore, the mass gain due to the massive copper electrodeposit, is shifted toward more negative values (Fig. 4 curve b′) indicating that the electrodeposition process of copper involved the displacement of ReO_4^- ion from the electrode surface.

Fig. 5 shows the j/t transient obtained from several potential steps of electrodeposition E_e (a–c) and the corresponding stripping voltammetry analysis (d–f) for the films formed after the potential steps onto glassy carbon substrates. The charges involved in these experiments are presented in Table 1.

In the case of the potential step carried out at an $E_e = -0.2$ V (Fig. 5a), a j/t transient that follows the Cottrell law is observed, with a charge value of 2.2 mC associated with the copper electrodeposition as is demonstrated by the stripping voltammetry in Fig. 5d, showing a single process corresponding to peak I_a in Fig. 1.

When the potential deposition is made more negative, $E_e = -0.500$ V (Fig. 5b), a slight increase in the current after approximately 15 s of the beginning the J/t transient is observed. This can be due to the first stages of rhenium deposition at this potential, and can be seen from the stripping curve (Fig. 5e), where the appearance of an anodic peak (namely II_a in Fig. 1), related to the $Re(0) \rightarrow Re(VII)$ reaction is detected. The same effect is more clearly observed when the step potential is made even more cathodic, $E_e = -0.560$ V (see Fig. 5c), where a clear nucleation and growth phenomena appears associated with the rhenium deposit, and in agreement with the increase of the stripping charge (see Fig. 5f) corresponding to increase of peak II_a in Fig. 1.

In order to study the influence of the copper presence in the nucleation and growth of rhenium ion, different experiments of potential steps were done onto copper, glassy carbon and gold electrodes. Fig. 6 shows the j/t response of different interfaces to which a step potential of −0.56 V has been applied. It can be observed that in the C/ReO_4^- interface rhenium begins to be electrodeposited after an induction time of 25 s. This time is relatively long compared with those obtained for the Cu/ReO_4^- and $C/Cu^{+2} + ReO_4^-$ interfaces. In the last case, we can assume that Re is deposited onto metallic copper since at this potential ion copper is reduced before the perrhenate ion. Furthermore, this effect has been demonstrated for the rhenium and copper electrodeposition on a gold electrode in nanobalance experiments, as is shown in Fig. 7. In this figure it can be seen that during the first 10 s the mass change indicates only copper deposition and after this time rhenium begins to be electrodeposited. These facts indicate that the induction time of nucle-

Table 1
Charge values involved in the potential steps and stripping analysis experiments done as is referred in Fig. 5, and for similar experiments done on a glassy carbon electrode, in a rhenium solution

E (V)	Q_e (mC)[a]	$Q_{s,T}$ (mC)[b]	$Q_{s,Cu}$ (mC)[c]	$Q_{s,Re}$ (mC)[d]
−0.20	2.2	2.2	2.2	0
−0.50	5.4	3.4	3.1	0.3
−0.56	12.0	4.7	2.9	1.8
−0.56[e]	4.3	0.45	0	0.45

[a] Cathodic charge of deposition.
[b] Total stripping charge.
[c] Copper stripping charge.
[d] Rhenium stripping charge.
[e] Rhenium solution (without copper).

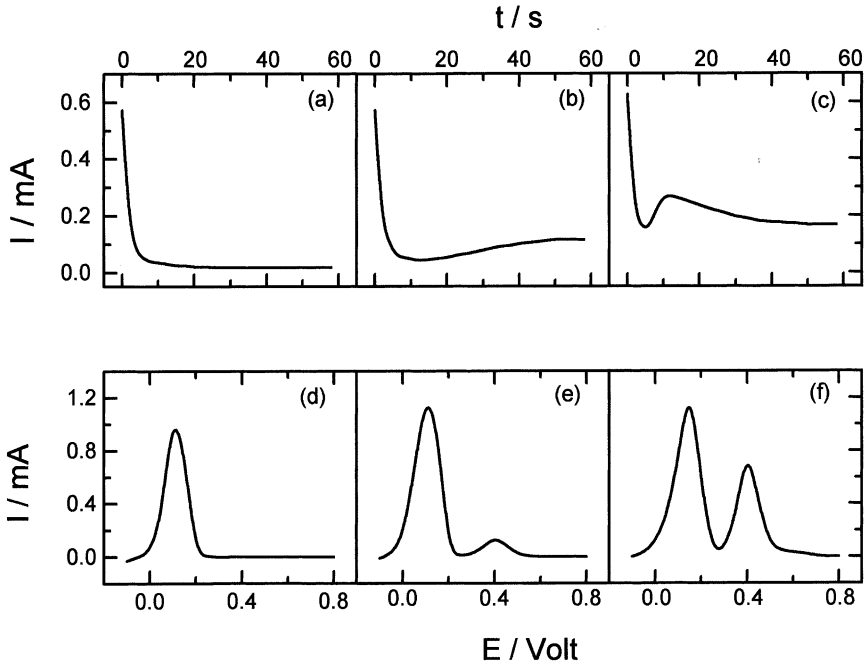

Fig. 5. Potentiostatic current–time transients recorded at a glassy carbon electrode in 6.25 mM $CuSO_4$ + 50 mM $HReO_4$ + 0.1 M Na_2SO_4 (pH 2) solution, at potential steps $E_e = -0.200$ V (a), −0.500 V (b) and −0.560 V (c). (d–f) are the corresponding stripping voltammograms done in 0.5 M H_2SO_4 solution. Sweep rate, 20 mV s^{-1}.

ation and growth process for rhenium is shorter in the presence of copper ions. This behavior can be explained in terms of the activation energy of the nucleation process onto the substrate that have been used. We propose a two-step nucleation process that can be expressed by means of the following formula:

$$S + ReO_4^- + 8H^+ + 7e^- \rightarrow SRe(ads) + 4H_2O \quad (1)$$

$$n\ SRe(ads) \rightarrow S[Re_n]_{nucleus} \quad (2)$$

where S and $S[Re_n]$ represent the substrate surface and critic nucleus that begin to grow, respectively.

The first step corresponds to those processes associated with the charge transfer and the ad-atom formation [Eq. (1)]; and the second step to the reorganization of these species interacting each other until the nuclei formation [Eq. (2)]. Therefore, the energy of activation of the second process [Eq. (2)] which is associated with the induction time, will depend on the stabilization degree of the rhenium ad-atoms onto the specific substrate. The mechanism proposed assumes that the rhenium ad-atoms will be more stable when they are deposited on glassy carbon than when they are deposited onto a copper electrode or electrodeposited copper thin film. This takes into account that functional groups containing oxygen, which are present on the glassy carbon surface, can interact with the rhenium ad-atoms. Thus, the activation energy for the rhenium nucleation process or the corresponding induction time, would be greater on glassy carbon substrates. This hypothesis would indicate that each element nucleates in an independent form and the type of alloy that is forming corresponds to a group of crystallites of both elements, which begin from pure nuclei.

The phenomenology observed by means of cyclic voltammetry and potential steps, give evidence that the co-deposition of copper and rhenium is possible. However, the type of alloy that both metals can form is not clear and will be discussed below from the X-ray diffraction data.

An increase of the current efficiency for rhenium

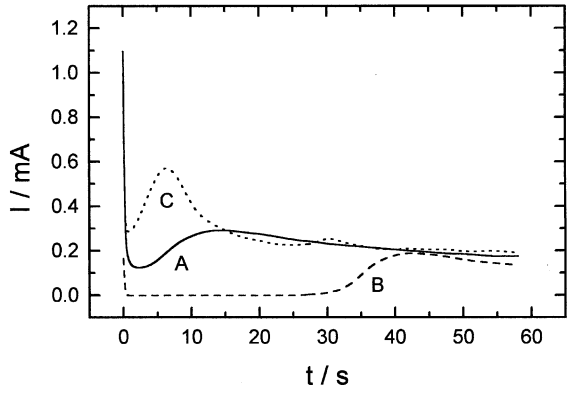

Fig. 6. Potentiostatic current–time transients recorded at a copper electrode in 50 mM $HReO_4$ (c), and at a glassy carbon electrode in 50 mM $HReO_4$ (b) and in 6.25 mM $CuSO_4$ + 50 mM $HReO_4$ (a). Supporting electrolyte 0.1 M Na_2SO_4 at pH 2. Potential step of −0.56 V.

electrodeposition when copper is electrodeposited from the same solution can be deduced from the following charge ratios, obtained from Table 1:

$$\left(\frac{Q_{s,Re}}{Q_e}\right)_{\text{with copper}} \geq \left(\frac{Q_{s,Re}}{Q_e}\right)_{\text{without copper}} \quad (3)$$

where $Q_{s,Re}$ is the rhenium stripping charge and Q_e is the cathodic charge of deposition.

The experimental results found in this work, despite the observed differences on the three employed substrates, indicate that it is possible to electrodeposit both Cu and Re with similar current efficiencies onto these different substrates. From deposition and stripping charges together with mass changes measurements, efficiency values between 93% and 96% for copper and 14–18% for rhenium were obtained. The low current efficiency for the rhenium electrodeposition is due fundamentally to the rhenium crystallites that are being electrodeposited, which electrocatalyze the hydrogen evolution reaction, and then, the major amount of the current is used in this process. When rhenium and copper are co-deposited, the current efficiency for the rhenium electrodeposition increases slightly, possibly due to the presence of copper adatoms on the rhenium crystallites, that inhibit the hydrogen evolution reaction.

Fig. 8 shows the effect of the electrodeposition potential on the composition of Cu–Re electrodeposited films deposited onto Ti substrates, as estimated by EDX. These results are consistent with the general trends for alloy deposition: the less noble component is deposited at higher overpotentials, thus the rhenium content increases as the electrodeposition potential is made more cathodic. However, films with only a 10% rhenium atomic fraction have been obtained in the −0.60 to −0.75 V potential range. This low rhenium content can be due to the low current efficiency at-

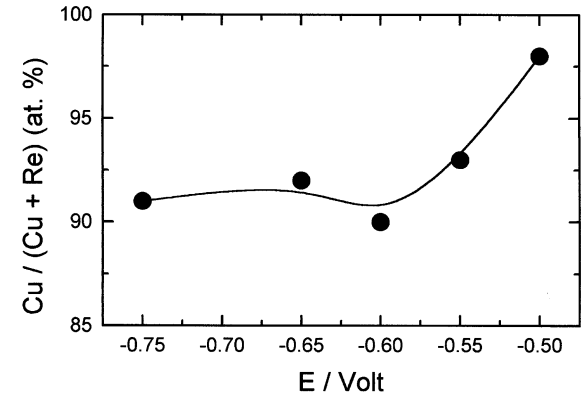

Fig. 8. The Cu/(Cu + Re) atomic ratio measured by EDX for films deposited at different potentials onto a titanium electrode from a solution containing: 6.25 mM $CuSO_4$ + 50 mM $HReO_4$ + 0.1 M Na_2SO_4 at pH 2.

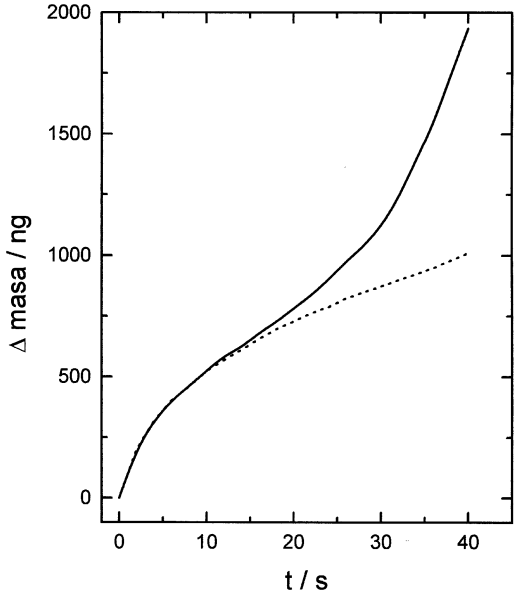

Fig. 7. Nanogravimetry analysis of copper (.....) and copper + rhenium (———) electrodeposition onto a gold electrode in 6.25 mM $CuSO_4$ and 6.25 mM $CuSO_4$ + 50 mM $HReO_4$ solutions, respectively. The potential was held at −0.56 V and the mass was continuously monitored as a function of time.

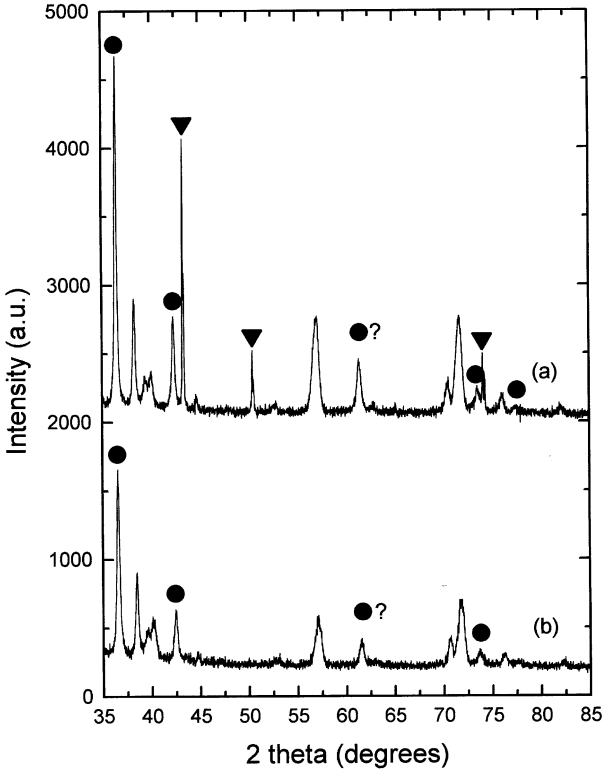

Fig. 9. X-Ray diffraction patterns of electrodeposited Cu–Re films of two different atomic compositions: (a) ~100% Cu and (b) ~90% Cu, obtained potentiostatically from a 6.25 mM $CuSO_4$ + 50 mM $HReO_4$ + 0.1 M Na_2SO_4 solution (pH 2) at $E = -0.500$ V and −0.750 V, respectively. (▼, Cu; ●, Cu_2O; ●? Cu_2O and/or CuO; peaks without labels correspond to the titanium substrate).

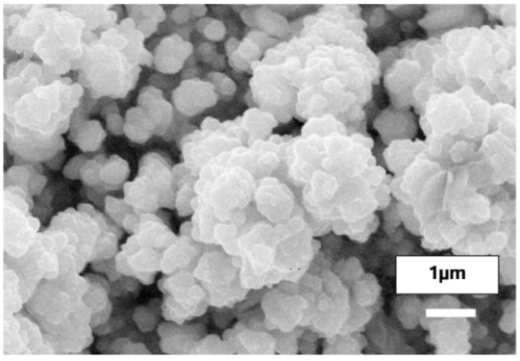

Fig. 10. SEM image of the top view of a Cu–Re thin film electrodeposited at a potential of −0.750 V vs. SCE.

tributed to the co-evolution of hydrogen, as was discussed above.

Fig. 9 presents the X-ray diffraction patterns for two representative Cu–Re film samples electrodeposited at −0.500 and −0.750 V. The film electrodeposited at −0.500 V, with an atomic composition of nearly 100% Cu, shows the diffraction peaks corresponding to copper and copper(I) oxide [12,13], in agreement with the EDAX analysis. The formation of copper(I) oxide is most likely a result of sample exposure to the laboratory ambient. However, the sample with 10% rhenium, shows only diffraction peaks corresponding to the copper (I) oxide phase. Moreover, the more intense diffraction peak of copper and those corresponding to the rhenium phase [14] are absent. So, we can assume that a micro-alloy of Cu–Re in a micro-crystalline state is being formed, hypothesis reinforced by the SEM study. Fig. 10 shows the scanning electron micrographs of an electrodeposited Cu–Re sample. The SEM examination revealed a highly irregular surface morphology comprising of granular-cauliflower and underlayer amorphous regions. The granular region, grain size of approximately 0.3–0.5 μm, presents faceted crystallites which probably correspond to the copper (I) oxide outer layer, but under this layer an amorphous phase can be seen.

4. Conclusions

The electrochemical behavior of copper, perrhenate and copper + perrhenate solutions onto glassy carbon, titanium and gold have been studied. The effect of substrate on the nucleation and growth has been investigated, and a possible mechanism for the perrhenate adsorption and nucleation has been proposed. Deposition onto titanium and carbon seems pretty similar, whereas for gold we conclude that adsorption effects are taking place. The main difference between the three electrodes studied here is the influence of the initial copper deposit. On gold, perrhenate adsorption displaces the copper deposition, but after the substrate has been covered by the alloy, we are basically using a copper electrode. Copper–rhenium alloys were electrodeposited potentiostatically onto titanium substrates from acidic solutions containing 6.25 mM $CuSO_4$ + 50 mM $HReO_4$ + 0.1 M Na_2SO_4 at pH 2. The rhenium content increases as the potential was made more cathodic, reaching a maximum value of 10% atomic composition. The films were micro-crystalline, and probably corresponded to a copper–rhenium micro-alloy.

Acknowledgements

The authors gratefully acknowledge financial support by Proyecto FONDECYT No. 1990675 and to the DGI-UCV. E.A.D. carried out this work with the support of the PEDECIBA-Física program which is kindly acknowledged.

References

[1] L.E. Netherton, M.L. Holt, J. Electrochem. Soc. 99 (1952) 44.
[2] V.P. Greco, W. Baldauf, P.J. Cote, Plating 61 (1974) 423.
[3] G.A. Jones, C.A. Faunce, D. Ravinder, H.J. Blythe, V.M. Fedosyuk, J. Magn. Magn. Mater. 184 (1998) 28.
[4] L.E. Netherton, M.L. Holt, J. Electrochem. Soc. 98 (1951) 106.
[5] A.A. Nikitina, Z.M. Sominskaya, A.T. Vagramyan, Zashchita Metal 1 (1966) 367.
[6] R. Schrebler, M. Merino, H. Gómez, R. Córdova, Meeting Abstracts of the 192th Meeting of the Electrochemical Society (MA 97-2), Paris, France, August 31–September 5, 1997, p. 1388.
[7] A.J. Bard, L.R. Faulkner, Electrochemical Methods: Fundamentals and Applications, John Wiley and Sons Inc, New York, NY, 1980.
[8] Ch. Wei, N. Myung, K. Rajeshwar, J. Electroanal. Chem. 375 (1994) 109.
[9] A. Marlot, J. Vedel, J. Electrochem. Soc. 146 (1999) 177.
[10] B.R. Scharifker, J. Mostany, M. Palomar-Pardavé, I. González, J. Electrochem. Soc. 146 (1999) 1005.
[11] H. Gómez, R. Schrebler, R. Córdova, R. Ugarte, E.A. Dalchiele, Electrochim. Acta 40 (1995) 267.
[12] JCPDS File 4-0836 (Cu), 1992.
[13] JCPDS File 5-0667 (Cu_2O), 1992.
[14] JCPDS File 5-0702 (Re), 1992.